

## First-principles study of electronic structure and optical properties of the LaAlO<sub>3</sub>/SrTiO<sub>3</sub> interfaces

M. J. Tang<sup>a</sup>, S. Q. Yang<sup>a,b,\*</sup>, T. H. Liang<sup>a</sup>, Q. X. Yang<sup>a</sup>, and K. Liu<sup>c</sup>

<sup>a</sup> Chengdu Polytechnic, Chengdu 610041, China

<sup>b</sup> State Key Laboratory of Electronic Thin Films and Integrated Devices, University of Electronic Science and Technology of China, Chengdu 610065, China

<sup>c</sup> College of Physics and Electronic Engineering, Sichuan Normal University, Chengdu 610066, China

Received 10 September 2012; Accepted (in revised version) 3 October 2012

Published Online 28 June 2013

---

**Abstract.** The electronic structure and optical properties of the perovskite oxide LaAlO<sub>3</sub>, SrTiO<sub>3</sub> and LaAlO<sub>3</sub> /SrTiO<sub>3</sub> interfaces were studied by the density functional theory (DFT) based on First-principles plane wave pseudopotential method. The energy band structure analysis shows that the (AlO<sub>2</sub>)<sup>-</sup> / (TiO<sub>2</sub>)<sup>0</sup> interface is insulating with the band gap being 1.888 eV, whereas the (LaO)<sup>+</sup> / (SrO)<sup>0</sup> interface seems to be a semiconductor or semimetal with the band gap being 0.021 eV. Moreover, we have also investigated optical properties of the LaAlO<sub>3</sub>, SrTiO<sub>3</sub> and LaAlO<sub>3</sub>/SrTiO<sub>3</sub> interfaces, the results indicate that the intensities of absorption, reflectivity, and energy loss spectra of LaAlO<sub>3</sub> and SrTiO<sub>3</sub> are higher than the corresponding intensities of the LaAlO<sub>3</sub> /SrTiO<sub>3</sub> interfaces.

PACS: O562.1

**Key words:** LaAlO<sub>3</sub>/SrTiO<sub>3</sub> interface, electronic structure, optical properties, first principles

---

## 1 Introduction

In recent years, the heterointerfaces of the perovskite oxide have been greatly studied because of their huge application for electronic devices, such as field-effect transistors, bipolar transistors, and light emitting diodes [1], and because of these perovskite oxides have simple atomic structures and rich physical properties, which can realize the change of magnetic - nonmagnetic, metallic - insulated by means of atomic change [2].

Ohtomo *et al.* [3] fabricated the atomic-scale LaTiO<sub>3</sub> (LTO)/SrTiO<sub>3</sub> (STO) heterointerfaces and observed the spatial distribution of the extra electron on the titanium sites even

---

\*Corresponding author. *Email address:* sqyang2004@yahoo.com.cn (S. Q. Yang)

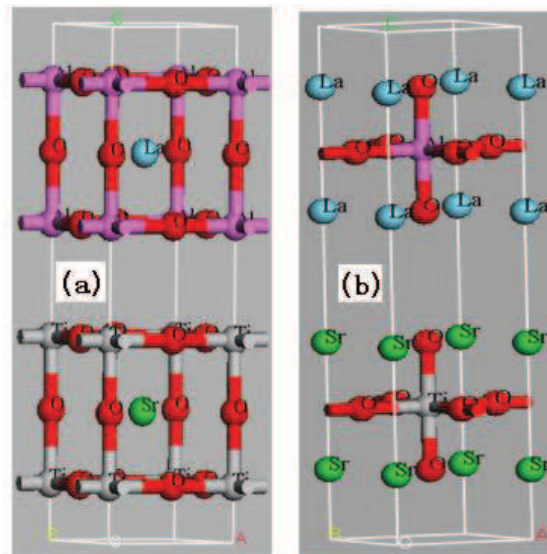


Figure 1: The interface structure configurations of LAO/STO (a)  $(\text{AlO}_2)^- / (\text{TiO}_2)^0$  interface; (b)  $(\text{LaO})^+ / (\text{SrO})^0$  interface.

though the superlattice structure is based on two insulators, and suggested that the extra electron could be driven by the presence of charged donor LaO layers. Later, Ohtomo and Hwang [4] found a high mobility electron gas at  $\text{LaAlO}_3(\text{LAO})/\text{STO}$  heterointerface and considered that the properties of interface is depend on the structure of the interface. The hole-doped interface  $(\text{AlO}_2)^- / (\text{SrO})^0$  (AO-SO) is found to be insulating, whereas the electron-doped interface  $(\text{LaO})^+ / (\text{TiO}_2)^0$  (LO-TO) is conducting. Nakagawa *et al.* [5] proposed a simple electrostatic model. Thiel *et al.* [6] suggested that the conductivity of the electron gases can be modulated through a quantum phase transition from an insulating to a metallic state. Meanwhile, various theoretical and experimental studies have attracted attention [7-16]. Until now, the electrical and optical properties of  $(\text{AlO}_2)^- / (\text{TiO}_2)^0$  (AO-TO) and  $(\text{LaO})^+ / (\text{SrO})^0$  (LO-SO) interfaces have been little known. Therefore, investigation into the electronic and optical properties of LAO/STO interfaces is relevant and intriguing.

## 2 Models and methods

The present calculations were performed with CASTEP code based on density functional theory [17]. All possible structures are optimized by the BFGS algorithm, which provides a fast way of finding the lowest energy structure. Further, the optimization is performed until the forces on the atoms diminish to less than  $0.05 \text{ eV}/\text{\AA}$ , and on all the stress components, to less than  $0.1 \text{ GPa}$ . The tolerance in the self-consistent field (SCF) calculation is  $2.0 \times 10^{-5} \text{ eV/atom}$ . Ultrasoft pseudopotentials are expanded within a plane-wave basis

set with a 300 eV cutoff energy level in the process of optimization, in which the orbits of O-2s<sup>2</sup>2p<sup>4</sup>Al-3s<sup>2</sup>3p<sup>1</sup>Ti-3d<sup>2</sup>4s<sup>2</sup>Sr-4p<sup>6</sup>5s<sup>2</sup>, La-5d<sup>1</sup>6s<sup>2</sup> are treated as valence electrons. Exchange and correlation effects are shown in the scheme of LDA-CA-PZ [18]. The  $k$  points sampling are  $3 \times 3 \times 1$ , according to the Monkhorst-Pack [19] method. The geometry of the superlattices is schematically shown in Fig. 1 for two kinds of interfaces with the  $(\text{AlO}_2)^- / (\text{TiO}_2)^0$  interface [Fig. 1(a)] and the  $(\text{LaO})^+ / (\text{SrO})^0$  [Fig. 1(b)] has one unit cells of both  $\text{LaAlO}_3$  and  $\text{SrTiO}_3$ . Since the different between the experimental lattice constants of  $\text{LaAlO}_3$  ( $a = 3.811 \text{ \AA}$ ) and  $\text{SrTiO}_3$  ( $a = 3.905 \text{ \AA}$ ) is small [4, 5], we use an average value ( $a = 3.858 \text{ \AA}$ ) of the experimental lattice constants. All superlattices are tetragonal unit cells, so we use lattice constants,  $a = b = 3.858 \text{ \AA}$  and  $c = 15.776 \text{ \AA}$ .

## 3 Results and discussion

### 3.1 Electronic properties

First, the electronic band structures of the  $\text{LaAlO}_3$ ,  $\text{SrTiO}_3$  and the interfaces of LAO/STO, where the top valence band is set at  $E = 0$ , are shown in Fig. 2. We can see that both  $\text{LaAlO}_3$  and  $\text{SrTiO}_3$  have direct band gap, with the top of its valence band and the bottom of the conduction band at the G point. The calculated energy gap of  $\text{LaAlO}_3$  is 3.189 eV which is less than the experimental measure (5.6 eV) [4], and the  $\text{SrTiO}_3$  is 1.835 eV, which is also less than the experimental measure (3.2 eV) [4]. Although theory tends to underestimate the energy gap, the relative value is still accurate.

In Fig. 2(c) and (d) we plot the electronic band structures of LAO/STO. The band gap of  $(\text{AlO}_2)^- / (\text{TiO}_2)^0$  interface is about 1.888 eV, it should be an insulator, whereas the  $(\text{LaO})^+ / (\text{SrO})^0$  interface is about 0.021 eV which seems to be a semiconductor or semimetal. Ohtomo and Hwang [4] reported that The hole-doped interface  $(\text{AlO}_2)^- / (\text{SrO})^0$  is insulating, whereas the electron-doped interface  $(\text{LaO})^+ / (\text{TiO}_2)^0$  is conducting. Therefore, it shows different electronic properties for various interfaces of LAO/STO.

### 3.2 Optical properties

We calculated in detail the interfaces of LAO/STO: optical properties, dielectric function, absorption coefficient, reflectivity, and electron energy-loss spectra.

The dielectric function is a very important parameter for a material because it is the fundamental feature of the linear response to an electromagnetic wave and uniquely determines the propagation behavior of the radiation within [20–22]. All other optical constants, such as the absorption coefficient, reflectivity spectra, and the electron energy-loss spectra could be deduced from the imaginary part  $\epsilon_2(\omega)$  and the real part  $\epsilon_1(\omega)$  of the dielectric function. The imaginary part,  $\epsilon_2(\omega)$ , can be given by calculating the momentum matrix elements between the occupied and unoccupied wave functions using selection rules, and the real part,  $\epsilon_1(\omega)$ , can be derived from  $\epsilon_2(\omega)$ , using the Kramer-Kronig relationship.

### 3.2.1 Dielectric function

The dielectric function of  $\text{LaAlO}_3$ ,  $\text{SrTiO}_3$  and the interfaces of LAO/STO are plotted in Fig. 3. For imaginary part, we can see that the total tendency of  $\text{LaAlO}_3$  and  $\text{SrTiO}_3$ , the interface of  $(\text{AlO}_2)^- / (\text{TiO}_2)^0$  and  $(\text{LaO})^+ / (\text{SrO})^0$  are similar. But the  $\text{LaAlO}_3$  is very different from the other three structures. Specifically, the imaginary part for  $\text{LaAlO}_3$ ,  $\varepsilon_2(\omega)$ , of the complex dielectric function is 0 in the range of  $0 \sim 4.5$  eV. However, the other three structures of  $\varepsilon_2(\omega)$  are not 0 within the same energy range. This difference originates from the fact that the optical transitions of electrons from VBs to CBs in the  $\text{LaAlO}_3$  acquire more energy. There is an excellent correlation between the dielectric function and the electronic band structures (Fig. 2);  $\text{LaAlO}_3$  has a large band gap (3.189 eV), but others have a narrow band gap in Fig. 2.

### 3.2.2 Absorption spectra, reflectivity spectra and loss function

Absorption spectra of the  $\text{LaAlO}_3$ ,  $\text{SrTiO}_3$  and the interfaces of LAO/STO are shown in Fig. 4(a). It is obvious that the absorption tendency of  $\text{LaAlO}_3$  and  $\text{SrTiO}_3$ , the formed

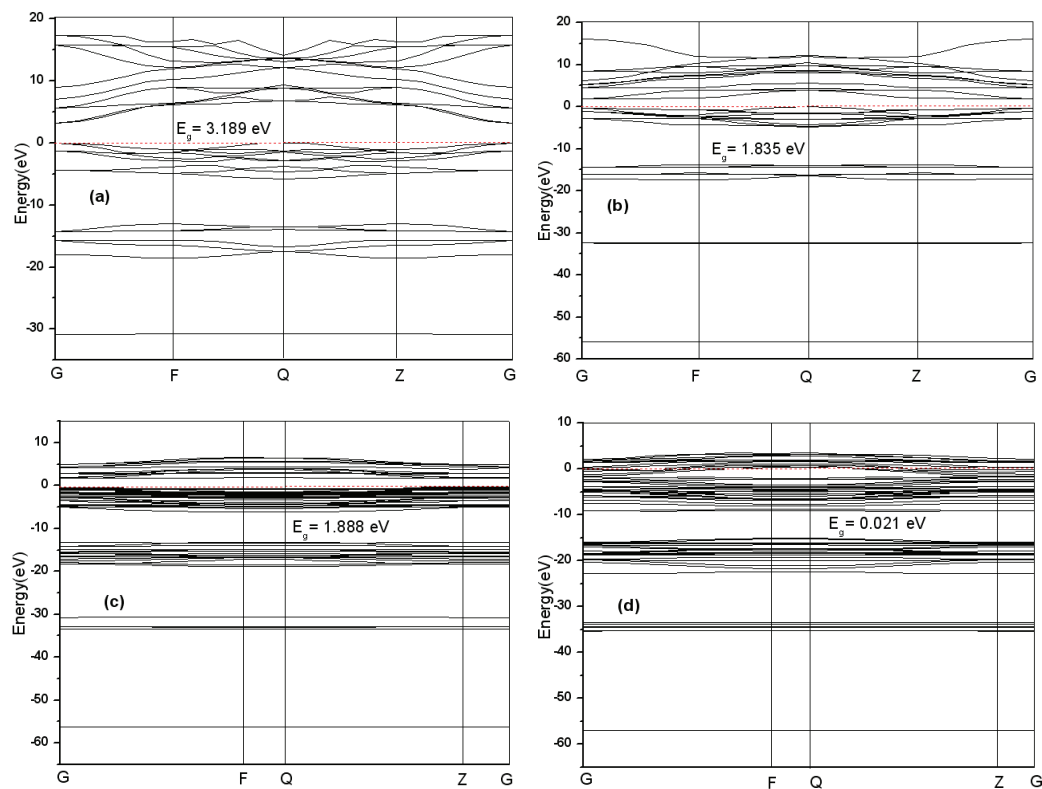


Figure 2: The band structure of (a)  $\text{LaAlO}_3$ ; (b)  $\text{SrTiO}_3$ ; (c)  $(\text{AlO}_2)^- / (\text{TiO}_2)^0$  interface; (d)  $(\text{LaO})^+ / (\text{SrO})^0$  interface.

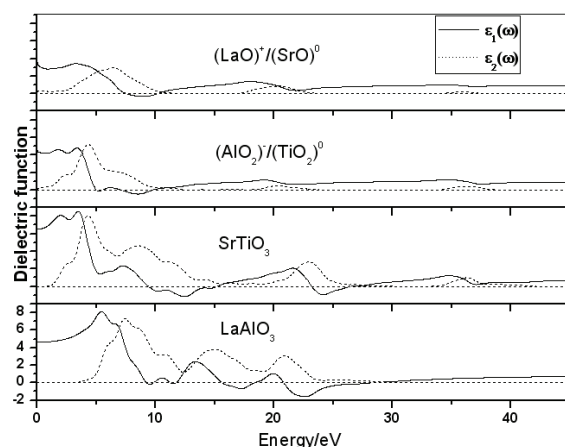


Figure 3: The calculated dielectric function.

interface of the  $(\text{AlO}_2)^- / (\text{TiO}_2)^0$  and the  $(\text{LaO})^+ / (\text{SrO})^0$  are similar. But the absorption intensity of  $\text{LaAlO}_3$  and  $\text{SrTiO}_3$  is larger than the two interfaces of  $(\text{AlO}_2)^- / (\text{TiO}_2)^0$  and  $(\text{LaO})^+ / (\text{SrO})^0$ , implying that attenuation of light of the two interfaces is weaker than  $\text{LaAlO}_3$  and  $\text{SrTiO}_3$ .

The calculated reflectivity spectra are shown in Fig. 4(b). The frequency and/or wavelength-dependent reflectivity indicates that all of the reflectivity coefficients are almost equal in the low energy region ( $0 \sim 11.3$  eV). In the high energy region ( $20 \sim 33$  eV), the reflectivity coefficients of  $\text{LaAlO}_3$  and  $\text{SrTiO}_3$  far outweigh that of the two interfaces, the reflectivity coefficient of  $\text{LaAlO}_3$  is the largest with 72%.

Fig. 4(c) shows the loss function  $L(\omega)$ , an important parameter describing the energy loss of a fast electron traversing the material. The peaks represent the characteristics associated with the plasma oscillation. The corresponding frequencies are the so-called plasma frequencies. It can be seen that there is a strong peak for  $\text{LaAlO}_3$  and  $\text{SrTiO}_3$  at about 26 eV, but the strong peak for the two interfaces is at about 10 eV, which corresponds to a rapid decrease of reflectance in Fig. 4(b).

## 4 Conclusions

The electronic and optical properties of  $\text{LaAlO}_3$ ,  $\text{SrTiO}_3$  and the interfaces of LAO/STO were investigated using the first-principles pseudopotential density functional method. The results show that all structures have a direct band gap, the  $\text{LaAlO}_3$ ,  $\text{SrTiO}_3$  and the interface of  $(\text{AlO}_2)^- / (\text{TiO}_2)^0$  should be insulators, the interface of  $(\text{LaO})^+ / (\text{SrO})^0$  seems to be semiconductor or semimetal. The dielectric functions and reflectivity, as well as the electron-energy-loss function were given in detail. To date, the direct comparison between the calculated results and the measured values remains difficult. However, our results may be still useful as experiment and references in the future.

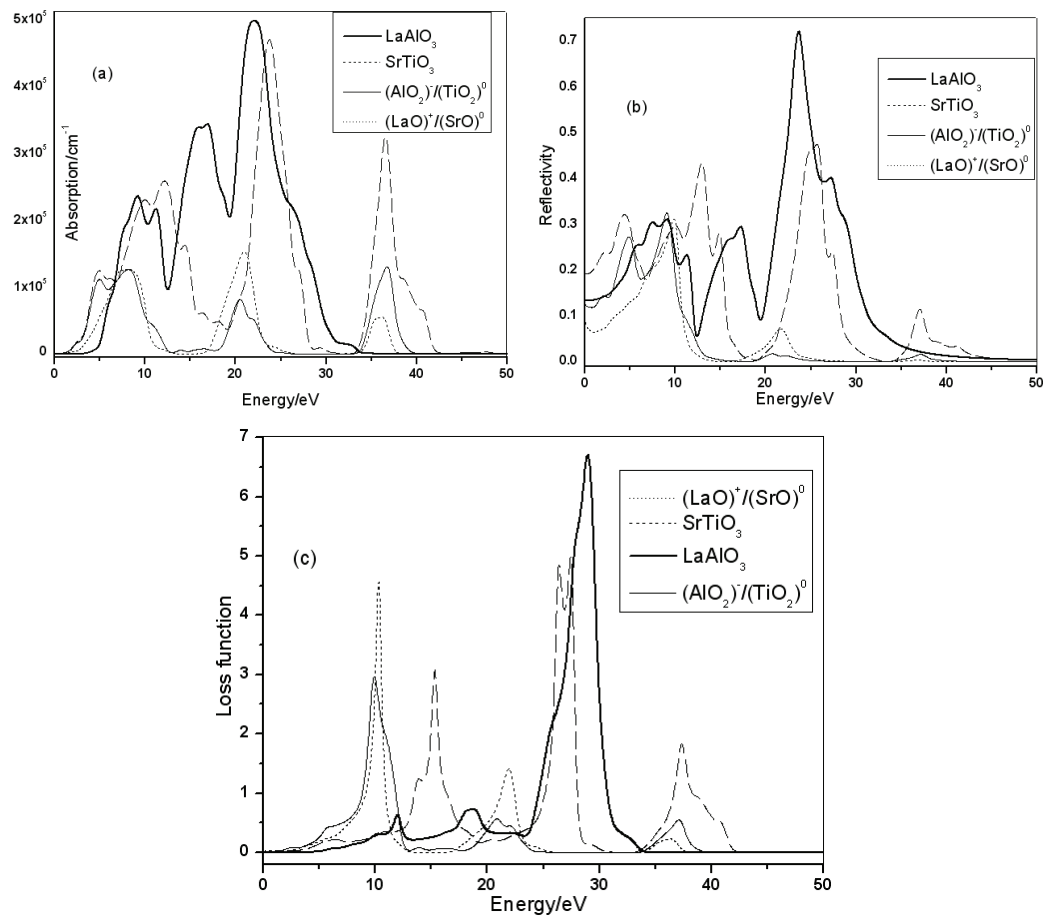


Figure 4: The calculated (a) absorption spectra; (b) reflectivity spectra; (c) energy loss function.

**Acknowledgments** The authors gratefully acknowledge the helpful discussions from W. X. Zhang and Y. R. Li. This work has been supported by the State Key Laboratory of Electronic Thin Films and Integrated Devices Program under Grant No. KFJJ200903.

## References

- [1] H. Kroemer, Rev. Mod. Phys. 73 (2001) 783.
- [2] J. G. Bednorz and K. A. Müller, Z. Phys. B: Condens. Matter 64 (1986) 189.
- [3] A. Ohtomo, D. A. Muller, J. L. Grazul, and H. Y. Hwang, Nature 419 (2002) 378.
- [4] A. Ohtomo and H. Y. Hwang, Nature 427 (2004) 423.
- [5] N. Nakagawa, H. Y. Hwang, and D. A. Muller, Nature Mater. 5 (2006) 204.
- [6] S. Thiel, G. Hammerl, A. Schmehl, *et al.*, Science 313 (2006) 1942.
- [7] M. Huijben, G. Rijnders, D. Blank, *et al.*, Nature Mater. 5 (2006) 556.
- [8] S. A. Pauli and P. R. Willmott, J. Phys.: Condens. Matter 20 (2008) 264012.

- [9] N. Reyren, S. Thiel, A. D. Caviglia, *et al.*, *Science* 317 (2007) 1196.
- [10] J. M. Albina, M. Mrovec, B. Meyer, *et al.*, *Phys. Rev. B* 76 (2007) 165103.
- [11] S. Gemming and G. Seifert, *Acta Mater.* 54 (2006) 4299.
- [12] K. Janicka, J. P. Velev, and E. Y. Tsybal, *Phys. Rev. Lett.* 102 (2009) 106803.
- [13] J. Lee and A. A. Demkov, *Phys. Rev. B* 78 (2008) 193104.
- [14] R. Pentcheva and W. E. Pickett, *Phys. Rev. Lett.* 102 (2009) 107602.
- [15] Z. S. Popovic, S. Satpathy, and R. M. Martin, *Phys. Rev. Lett.* 101 (2008) 256801.
- [16] H. Chen, A. M. Kolpak, and S. Ismail-Beigi, *Phys. Rev. B* 79 (2009) 161402(R).
- [17] W. Kohn and L. J. Sham, *Phys. Rev. A* 140 (1965) 1133.
- [18] N. LANG: in *Theory of the Inhomogeneous Electron Gas*, eds. S. Lundqvist and N. March, (Plenum, New York, 1983).
- [19] H. J. Monkhorst and J. D. Pack, *Phys. Rev. B* 13 (1976) 5188.
- [20] X. F. Li and Z. L. Liu, *J. At. Mol. Sci.* 3 (2012) 78.
- [21] J. M. Xie, *J. At. Mol. Sci.* 2 (2011) 342.
- [22] M. J. Tang, D. W. He, and L. He, *Physica B* 406 (2011) 3154.